Sci. J. Fac. Sci. Minufia Univ., 2009, Vol. XXIII, 55-74

STATISTICAL MODELING OF SEISMICITY PATTERNS BEFORE AND AFTER DAHSHOUR EARTHQUAKE, EGYPT

SAYED S. R. MOUSTAFA AND ADEL M. E. MOHAMED
Department of Seismology, National Research Institute of Astronomy and Geophysics, Helwan, Cairo, Egypt

ABSTRACT

On 12 October 1992 a moderate earthquake with magnitude, M_b =5.8 shocked the Dahshour area southwest of Cairo City, Egypt. A number of aftershocks accompanied the main event. Destructions caused by this event were concentrated in Cairo City, the Nile Valley and the Nile Delta areas. The aftershock sequence was remarkable in that it broke a region previously considered to be of low seismicity. This paper studied the seismicity during the period 1978-1997 by applying the Epidemic Type Aftershock Sequence (ETAS) model to the data. The whole period is divided into three stages: early background and relatively quiescent period, mainshock and aftershock sequence period, and active period of post-aftershocks. The paper discusses the different aspects of aftershock sequence including background, spatial-temporal analysis, ETAS model, relative quiescence, and its application to the recorded data.

Keywords: Dahshour earthquake; seismicity statistical modeling; ETAS model; point process; Egypt.

INTRODUCTION

During a sequence of earthquakes, the biggest energy is usually released by the mainshock. It could be preceded by foreshocks and followed by aftershocks (Mogi, 1969). Statistical studies related to the seismicity and occurrence of earthquakes could give us useful information to explain better the mechanism of seismicity. Many standard statistical tests, which have been employed, for the estimation of anomalous seismicity changes require declustering of the earthquake catalog in advance. However, by eliminating the clustered seismicity some useful information is lost from the resulting data apart from the imperfections of the

* Corresponding author. Tel.: +20 25560645
E-mail address: sayed.moustafa@gmail.com (S. Moustafa)

declustering algorithms themselves (Ogata, 1999). To circumvent such problems, Ogata (1985; 1988) developed the Epidemic Type Aftershock-Sequences (ETAS) model for seismicity analysis. The basic idea behind the model is to consider that each earthquake has its own set of aftershocks and to model the process by using the Modified Omori law and the relation between aftershock productivity and the magnitude of the mainshock (Ogata, 1999). The deviations of real data from the model once measured could reveal the possible precursory seismicity changes.

On 12 October 1992, an earthquake with magnitude M_b = 5.8, occurred in Dahshour area, southwest of Cairo, Northern Egypt (solid star in Fig. 1). This was the largest earthquake known to have occurred in this area since the historical destructive earthquake of August 1848 (Badawy, 1999). The epicenter was located in an area with no reported history of earthquakes during the last hundred years. However, after the installation of a temporal network (Abou El-Enean, 1993) immediately after the mainshock, numerous aftershocks were recorded. The Dahshour earthquake caused extensive damage in Cairo wherein 561 lives were lost, while several of the inhabitants were injured. More than 8300 buildings were damaged or destroyed. As a result, more than 2000 people became homeless (Hussein et al., 1996).

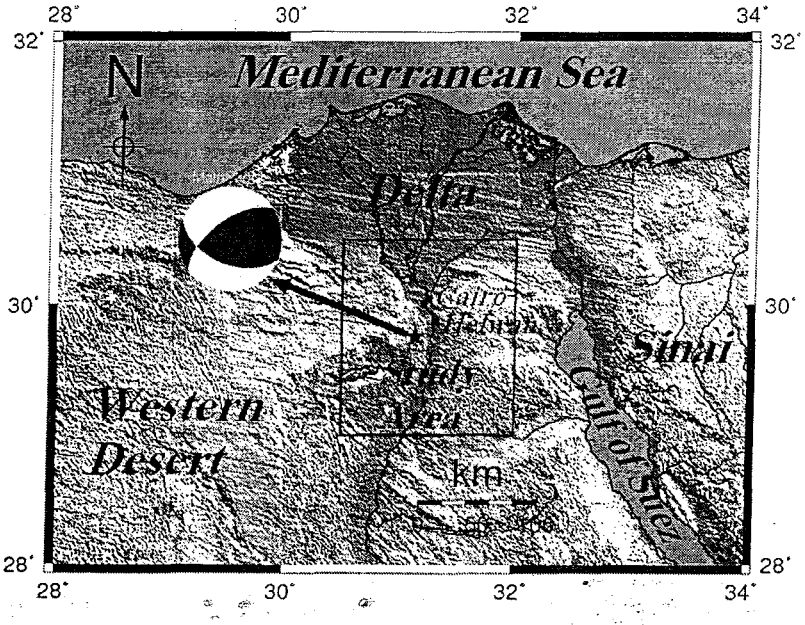

Fig. 1: Location map of the studied area (Solid rectangle). Solid star shows the location of the 12 October 1992 Dahshour earthquake epicenter, while the ball shows the focal mechanism of that event (After Hussien, 1999).

The main purpose of this study is to analyze the Dahshour earthquake aftershock sequence, particularly in relation to their fit with Omori law (Omori, 1894). This law and its modified forms, which describe the decay of aftershock activity with time, have been used widely as a fundamental tool for studying aftershocks (Utsu et al., 1995). Another task is to study the seismicity patterns in the region before and after the sequence. For this purpose, the ETAS model (Ogata, 1983, 1988, 1989, and 1992) was used. In its various forms, the ETAS model seems to be the best available representation of the main features of seismicity. It is a stochastic version of the modified Omori law. Based on the theory of branching processes or self-exciting point processes, it has only six independent parameters that can be used to describe both background activity and multistage aftershocks (Ogata, 1999).

REGIONAL AND LOCAL TECTONIC SETTINGS

The present day tectonic deformation within the selected study area is related to the regional tectonic forces and the local tectonics of Egypt (Fig. 2). The main regional tectonic framework of Egypt is divided into three regions where the main earthquake activity normally occurred. The first one is the African–Eurasian Plate margin where the African and Eurasian plates converged across a wide zone in the northern Mediterranean Sea. The earthquake activity is contained in a belt parallel to the Hellenic and Cyprian arcs. Some of the largest events located to the south of Crete and Cyprus Islands were felt and had caused several damages on the northern part of Egypt particularly the 1303 August 8, 1756 February 13, 1926 June 26, and 1996 October 10 earthquakes. The second tectonic region is the Red Sea plate margin. The earthquake activity in this region is related to plutonic activity reflected by the Red Sea rifting and the intersection points of the NW Gulf of Suez-Red Sea Faults with the NE Levant-Aqaba Faults. The extension of this deformation zone toward the north (Suez-Cairo shear zone) is considered to be the most active part in Northern Egypt (Kebeasy, 1984; Ben-Avraham et al., 1987; and Abou El-Enean, 1993). The larger earthquakes along this zone caused some damages to the northern part of Egypt that include the 1879 July 11 and 1900 March 6 Gulf of Suez earthquakes as well as 1969 March 31 Shadwan Island tremble. The last tectonic region encompasses the Levant Transform Fault. The larger events in this region that were reported with attendant damages in Northern Egypt occurred on 1068 March 18, 1202 May 20, and 1995 November 22 (Abou El-Enean, 1997).

From the satellite imagery (El-Shazly et al., 1979), the available geological maps (Egyptian Geological Survey, 1981), and the geological studies (Said, 1981

and El-Gamili, 1982), Miocene-Oligocene-Eocene sediments covered the epicentral area of the 1992 earthquake. No surface tectonic lineaments have been observed in the epicentral area (El-Shazly et al., 1979) which may probably be due to the thick loose sedimentary cover. However, on both sides of and close to the Nile River, a large number of NW-SE and NE-SW faults have been observed. The Egyptian Geological Survey and Mining Authority (EGSMA, 1993), concluded that the tectonic faults that affected the studied area are the Gulf of Suez NW-SE trends represented by Qatrani fault and the Mediterranean E-W trend represented by Gabal El-Sheeb fault. Majority of the surface fractures following the October 12, 1992 earthquake were directed mainly E-W.

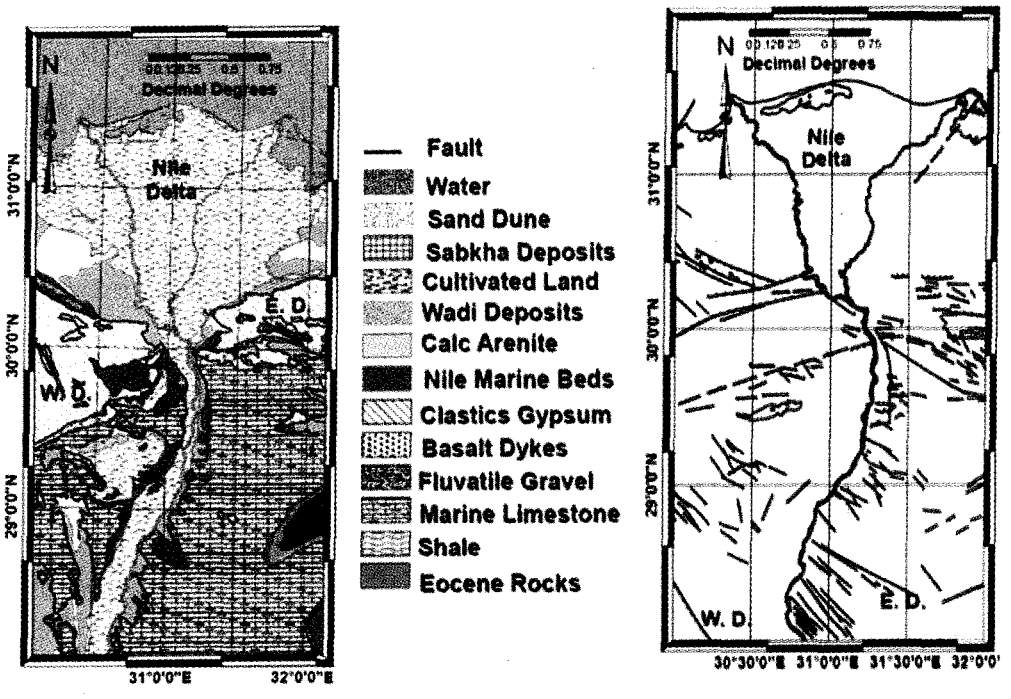

Fig. 2: The surface geology (left panel,) and surface and subsurface faults (right panel), of the study area (after the Egyptian Geological Survey and Mining Authority (EGSMA), 1981).

DATA

The earthquake catalog data used in this study were collected for the area limited by latitudes 28.5o-31oN and longitudes 30o-32oE (solid rectangle in Fig. 1) from the Egyptian catalog (Abou El-Enean, 1993, 1997). To construct the sequence only shocks shallower than 40 km were considered to accommodate full information on the sequence. Magnitudes were referenced with respect to the local

magnitude, M_L (Maamoun et al., 1984) empirical relation. One thousand two hundred and ten (1210) earthquakes of $M_L \geq 1.0$ from 25 January 1978 to 30 November 1997 (Fig. 3) were collected and assessed. Much effort was made to insure the completeness of the used catalog. However, still some incompleteness in the catalog exists. Especially for the periods from 1978 to 1992 and 1994 to 1997 due to lack of instrumentation in Egypt as a whole and particularly in the study area, because it was considered to be a low seismicity zone before the 1992 event. Among the 1210 events that were analyzed, the data set contains 69 events from 1978-1992 and 800 events from 1992-1993 due to the installation of a temporary seismic network just after the 1992 Dahshour earthquake deployed for about two years from October, 1992 to the end of 1994 (Abou El-Enean, 1993). Only two events were used in the catalog from 1994-1997 with magnitude of 3.5 that could be detected by regional networks around Egypt. Because completeness of the catalog is one of the most important issues to be considered in order to obtain reliable results in any seismicity-related study, this study is mainly based on 691 events with $M_L > 1.5$ as depicted in Fig. 4c

SEISMICITY ANALYSIS THROUGH POINT-PROCESS MODELING

The occurrence time of an earthquake can be considered a point process. Suitable modeling of the conditional intensity function of a point process is useful for the investigation of various statistical features of seismic activity. Following the theoretical concepts given by Zhuang (2003) this section summarizes the likelihood-based methods of analysis of point processes, and reviews the useful models of seismicity considered in our investigation of Dahshour area.

As defined by Omori (1894), the rate of aftershock $\lambda(t)$ decay is nearly proportional to the inverse of the time t elapsed after the main shock as represented by:

$$\lambda(t)=\frac{K}{t+c} \tag{1}$$

Where: K is a constant that depends on the total number of aftershocks in the sequence and c is the temporal shift. Utsu (1961) proposed a modification of the Omori model wherein:

$$\lambda(t)=\frac{K}{(t+c)^p} \tag{2}$$

Where: p and c are free parameters that can be estimated from the data, maximizing the likelihood function of the process (Ogata, 1983). Such power-law behavior is indicative of a physical process generally slower than those typically observed in nature usually described by negative exponentials (Utsu et al., 1995). The role of the two free parameters of the modified Omori model is rather different. While p has been introduced by Utsu (1961), to model sequence behaviors significantly deviating from a hyperbolic decay, the inclusion of c was essentially an algebraic expediency to avoid the fact that the rate tends to infinity for t approaching zero (Gross and Kisslinger, 1994; Narteau et al., 2002). Usually, the parameters p, c, and K of the modified Omori model are estimated using the maximum likelihood method, which makes it possible to practically forecast the probability of large aftershocks.

Extending the modified Omori model further, Ogata (1985, 1988, 1989), demonstrated that the ordinary seismic activity of a wide region could be described well in terms of the conditional intensity, by the superposition of a constant rate for background seismicity and by the modified Omori functions of any shock i which occurred at time t_i, such that:

$$\lambda(t_t)=\mu+\sum_{t_i<t}\frac{K_i}{(t-t_i+c)^p} \tag{3}$$

where: μ is an occurrence rate for the background seismic activity. The sum $\sum_{t_i<t}$ is taken for all shocks i, which occurred before time t. The parameter K_i for each shock i contribute to the size of the corresponding offspring or aftershock in a wide sense. The p value indicates the decay rate of aftershocks. The crucial point of the model here is that the parameter K_i is dependent on its magnitude M_i as well as the cut-off magnitude M_0 of the data set according to the following exponential function form:

$$K_i = K_0\, e^{\alpha(M_i-M_0)} \tag{4}$$

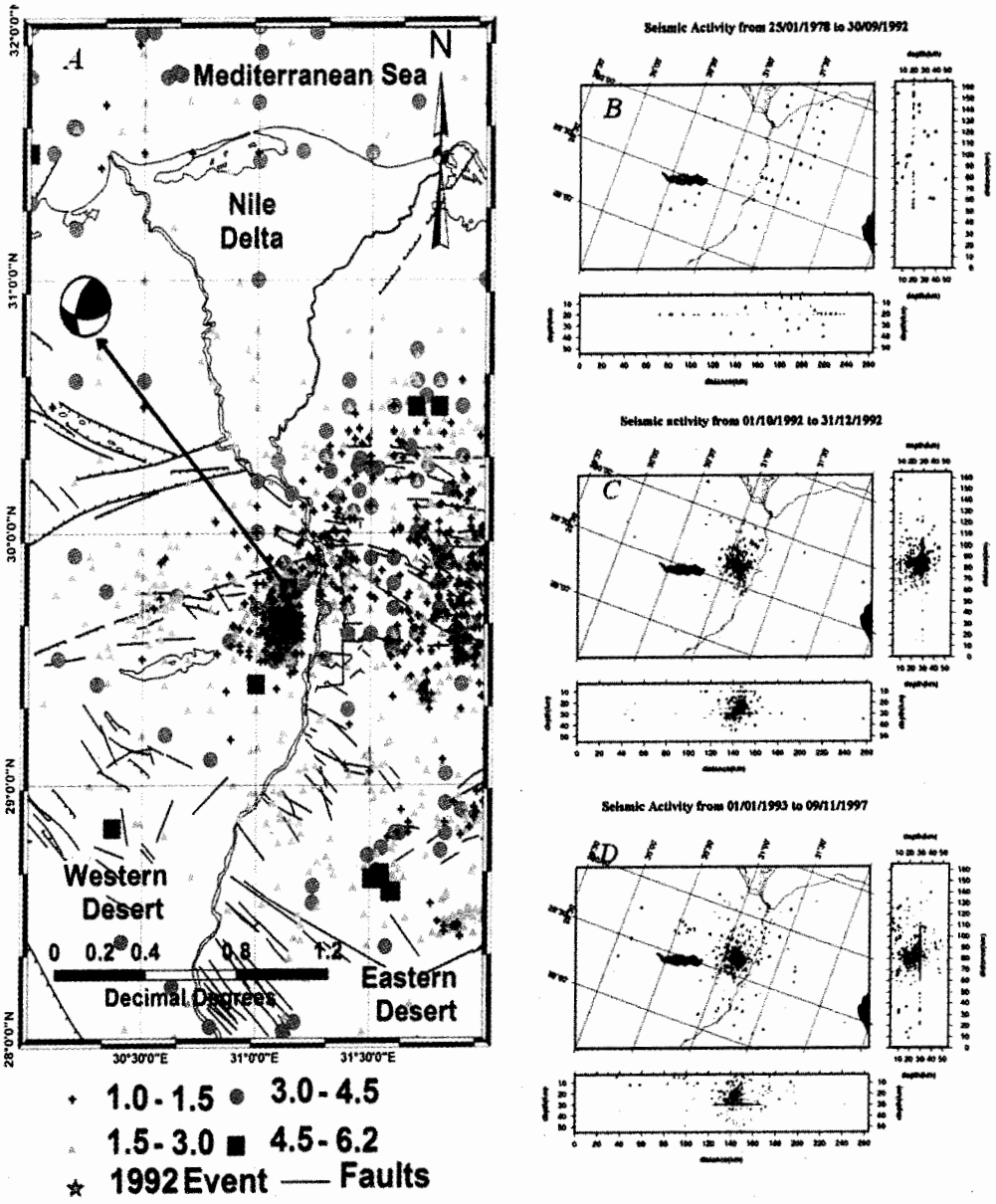

Fig. 3: a-Epicenter distributions of the Dahshour region (left panel). b- Epicenter distribution of the 691 earthquakes used in this study (right panel) recorded in Dahshour Region from 1978 to 1997. Right and bottom plots are the depth cross-sections for the whole events considered. The x-axis is the epicentral distance from the edge of the fault in km while the y-axis is the focal depth in km. The projection plane is vertical and perpendicular to the Dahshour fault. The different sized circles indicate different magnitudes.

This form is based on the empirical formula obtained by Utsu and Seki (1955) on the linear relation between the logarithms of aftershock areas and the magnitudes M of the mainshock (Utsu, 1971). Combining equations (3) with (4) for the ordinary seismicity in terms of the occurrence rate of shocks is called *Epidemic Type Aftershock-Sequences (ETAS)* model.

ANALYSIS AND RESULTS

Aftershock sequences offer a rich source of information on the Earth's crust and source properties of large earthquakes mainly because a very large number of events occur over a short period in a relatively small area. Aftershocks also pose a significant seismic hazard, which, under certain circumstances, can exceed those from the main shock hazard. In our analysis of the direct aftershock sequences, a non-stationary Poisson process with the rate proportional to the known Omori law was used. In the analysis of the periods prior and subsequent to the main aftershock sequence, the ETAS model was utilized to study the rates of occurrence and levels of clustering in the background activity. The Akaike Information Criterion (AIC) model selection procedure (Akaike, 1977) was employed for the best fits. In this procedure, models with different forms and parameters were compared by statistical computation using the equation:

$$AIC = -2\log L + 2k \qquad (5)$$

where: L is the likelihood and k is the total number of fitted parameters for the particular model being assessed. The model with smallest AIC is considered to be the best fit to the data.

1. Main features of Dahshour earthquake sequence

To study the main features of seismicity in the studied area, the whole time interval was divided into three periods. They are: (i) 1978.1.25-1992.9.30 (P1), (ii) 1992.10.1-1990.12.31 (P2), and (iii) 1993.1.1-1997.9.30 (P3). P1 has 58 events as shown in Fig. 3b. P1 could show background seismicity patterns and can be regarded as a preparation period of the mainshocks. P2 has 320 events as shown in Fig. 3c. This is the period of the immediate aftershock sequence. P3 has 313 events as shown in Fig. 3d. This is the post-aftershock period. Even at the end of P3, the rate is still much higher compared to P1. All earthquake events considered has a magnitude M_L>1.5. The majority of seismic activity in P1 was mainly concentrated on the northeast from the epicenter of the main event represented by a triangle in Fig. 3b. The direct aftershock sequence occurred in P2 and formed a group in space clustered around the main event. For the last period, P3, the pattern is less clustered than P2. The main activity took place along the

northeast-southwest-trending belt (NNE to NE direction), somewhat to the south of the main event. The general activity level is much higher than P1. Depth cross-sections for different time periods are shown in the right side and the lower sections of Fig. 3. The magnitude threshold used for these cross-sections was M_L>1.5. The section plane is parallel and perpendicular to the fault line of Dahshour fault. Its intersection with the Earth's surface has an azimuth of 70°. We did not try to extend our catalog until now using the data recoded by the Egyptian National Seismological Network (ENSN), because of the different magnitude scales used and no reliable relation between M_L used in our study and current used magnitude

According to Kebeasy (1990), this line represents the local activity zones namely, the Baharia-Fayum-Abu Roash-Cairo. It should be noted that the 12 October 1992 event took place within this zone. The large proportion of the two main clusters (Figs. 3c & 3d) are all beneath 20-35 km of depth. In the first period, earthquakes occurred mainly to the east and northeast of the main shock with an average depth of 20 km. The earthquakes in the direct aftershock sequence formed one cluster. The events in this period (Fig. 3c) were highly clustered, with an average depth of 13 to 33 km. In the final period, the events were located to the south and west of the main shock and remained to be explosive clusters by nature (Fig. 3d). From the magnitude-time plots (Fig. 4a), it was observed that, apart from the sequence itself the pattern of seismicity in the study area could be divided into three stages: average, quiet, and active. From the depth histogram plot (Fig. 4e); most of the events are at a depth of 10-33 km. To investigate the changing seismicity patterns with time, Gutenberg-Richer relation plot was drawn. The horizontal axis represents magnitude of events while the vertical axis represents the cumulative number (Fig. 3c). The cut-off magnitude was M_L > 1.5. However, caution must be taken in interpreting that figure, due to the incomplete earthquake data catalogue in the period 1983-1992 as previously mentioned. Before 1992, events were concentrated near the boundary of a circle of radius 30-50 km centered on the mainshock's epicenter.

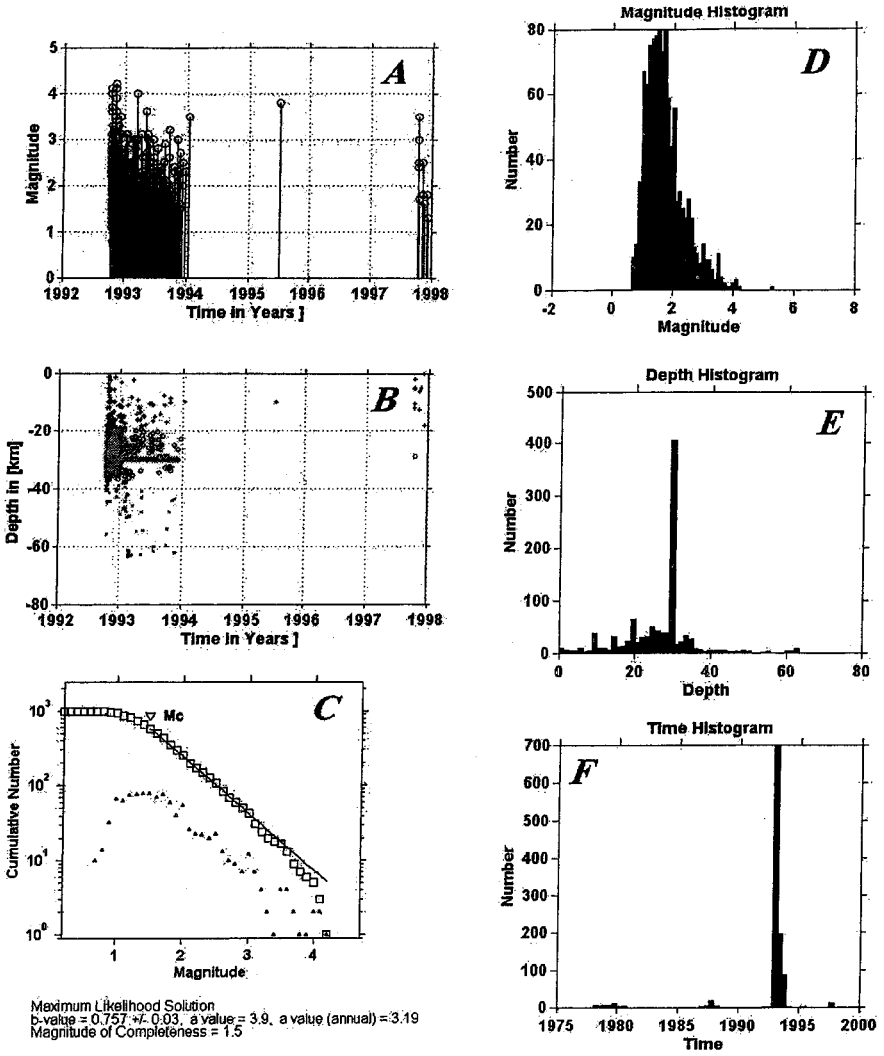

Fig. 4. Basic analysis of the seismicity in the Dahshour region. (a), Magnitude-time plot of events ML > 1.5. (b), time- depth plot of events ML > 1.5. (c), Gutenberg-Richter relation. (d), Magnitude histogram of events ML > 1.5. (e), Bar plots of depth distribution of events ML > 1.5. and (f), time histogram of events ML > 1.5.

2. Application of the Omori law and ETAS model to Dahshour earthquake aftershock sequence

2.1. Studies on the direct aftershocks

To study the properties of the direct aftershock sequence, the software tool zmap was used to give the general features of the direct aftershocks as depicted in Fig. 5. First plot shows the aftershocks cumulative number with time and explain the increasing rate of events until 1994, while the second and third plots show the direct application of Omori law (eq. 2) and give the free parameters of seismicity changes. The obtained values of p ranges from 0.24 to 0.31, values of c ranges from 0.545 to 0.835 and the value of k ranges from 10 to 11.9. The fourth plot explain the changes of seismicity with days and the last two plots give the range a- and b-values with respect to the number of earthquakes recorded.

Moreover, a comparison was made by fitting the Omori law and the ETAS model to events with $M_L > 1.5$. Here, the simple Omori law (Eq. 1) is first considered. The model with smallest AIC is considered to be the best fit to the data. The numerical results are shown in Table 1 and drawn in Figs. 6a and 6b wherein the ETAS model and several versions of the Omori law were applied to the data. All the models fit into the data over time intervals of 30, 50, and 90 days. From Table 1, it could be observed that the ETAS model gives the minimum AIC value and fits into the data more accurately compared to the other models. Although the Omori law accommodates more parameters than the ETAS model, the flexible nature of the later to change its conditional intensity as events occurred may be largely responsible for the more accurate data fit.

2.2. Existence of distinct seismic phases

Different combinations of models and periods were examined to determine the best combinations that fit into the data. Using the division into time intervals P1-P3, we fit the ETAS model for (a) the whole time interval, (b) the three periods separately, and (c) some intermediate combinations. To provide a reference for the improvements made by the ETAS model, the Poisson model is fitted at the same time, as shown in Tables 2 and 3. The comparison between AICs is given in Table 4.

From these tables and Fig. 6, it is observed that the ETAS model gives reliable and more accurate results than the Poisson model. The values of ΔAIC per event range from 0.0383 to 6.5804, which can be regarded as a big improvement for data fitting.

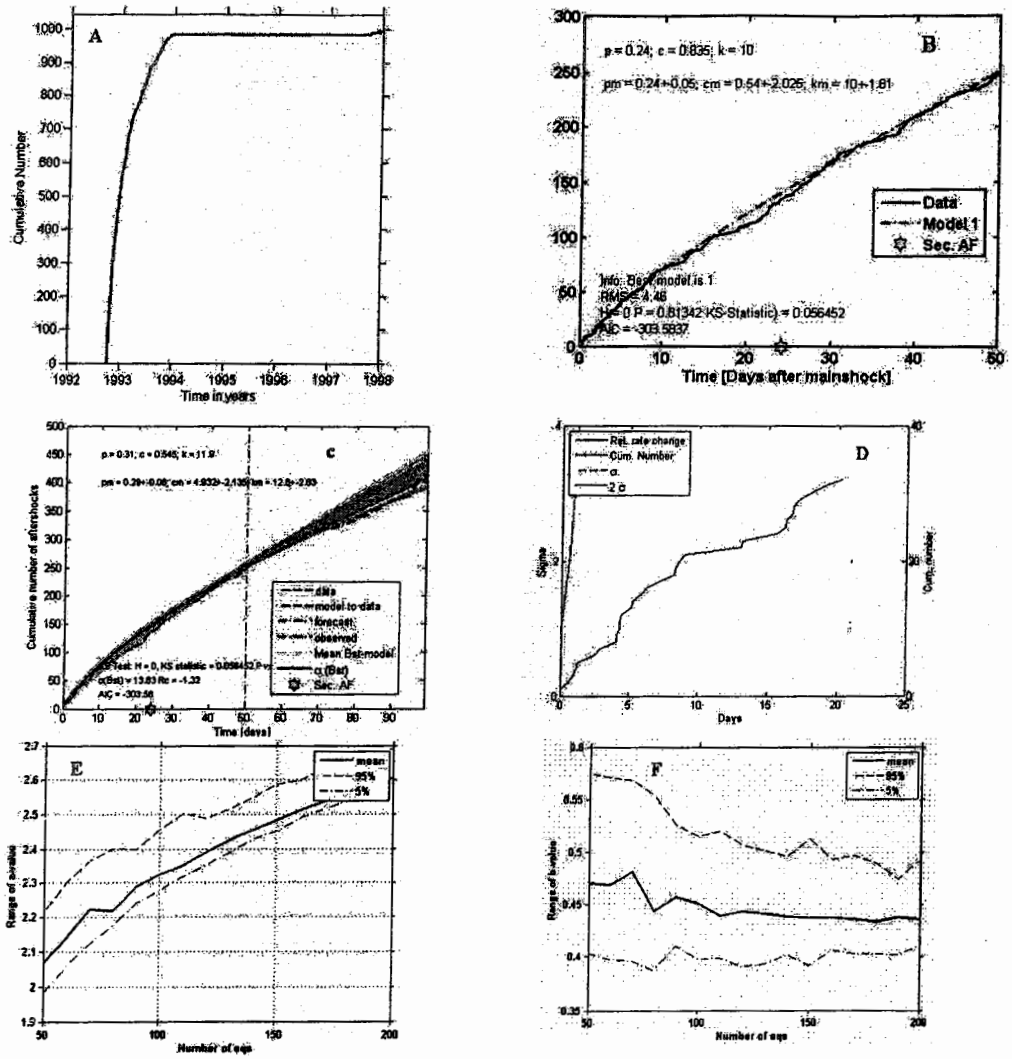

Fig. 5: general features of aftershock sequence of the 12 October, 1992 Dahshour earthquake.

Using one dividing point only, the best subdivision point for the subperiods is after the main shock, which makes a net substantial improvement in AIC of about 45.7. By dividing the whole time interval into three subperiods, the best model from the various combinations for the subdivision is that of three separate subperiods, which results in an improvement of 58.2 for AIC. For the subdivision of direct aftershocks and post-aftershocks, the change of AIC values is 13. The background seismicity rate (μ) of 0.001102 events/day in P1, increases

to 0.830285 events/day in period P2, and drops back to its original level of 0.003624 events/day in P3. The α values are approximately 0.3 in the periods P1 and P3, which indicate a seismicity pattern of ordinary swarms, whereas in P2 α = 0.632634, which indicates a pattern of foreshock swarms.

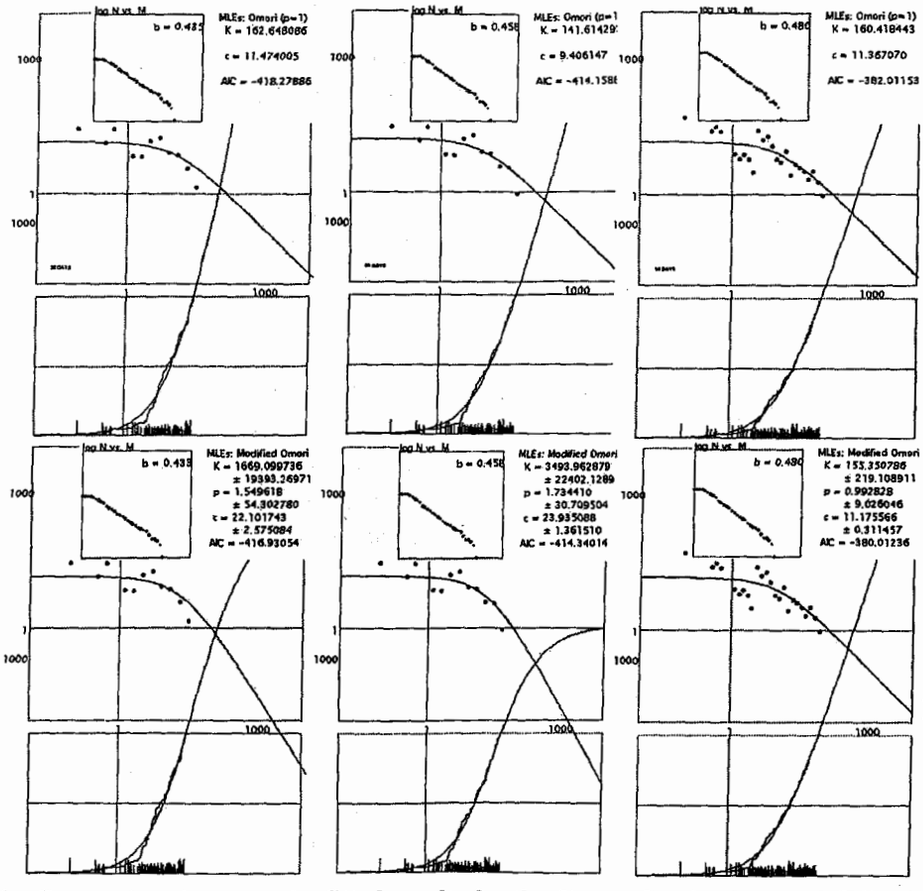

Fig. 6a. Comparison between the fitted results for the direct aftershock period (P2) with the Omori (upper plot) and Modified Omori (lower plot) statistical models for the periods of 30, 50, and 90 days respectively. The upper part of each plot shows the Gutenburg-Ritcher curve and the obtained b-value, various model constants and AIC values.

This correlated with the fact that the period P2 differs from the background period P1. The parameter c reaches its highest value of 0.125782 day in P3. A higher c value suggests that the events in a cluster are more spread out in time. The p values in each period were 3.0, 1.11, and 2.51 respectively. This suggests a change of the decay rate of aftershocks for the final period after the

main event. The *b*-values of 0.30288, 0.51018, and 0.50339 (see Fig. 5f) reflect the changes in magnitude structure.

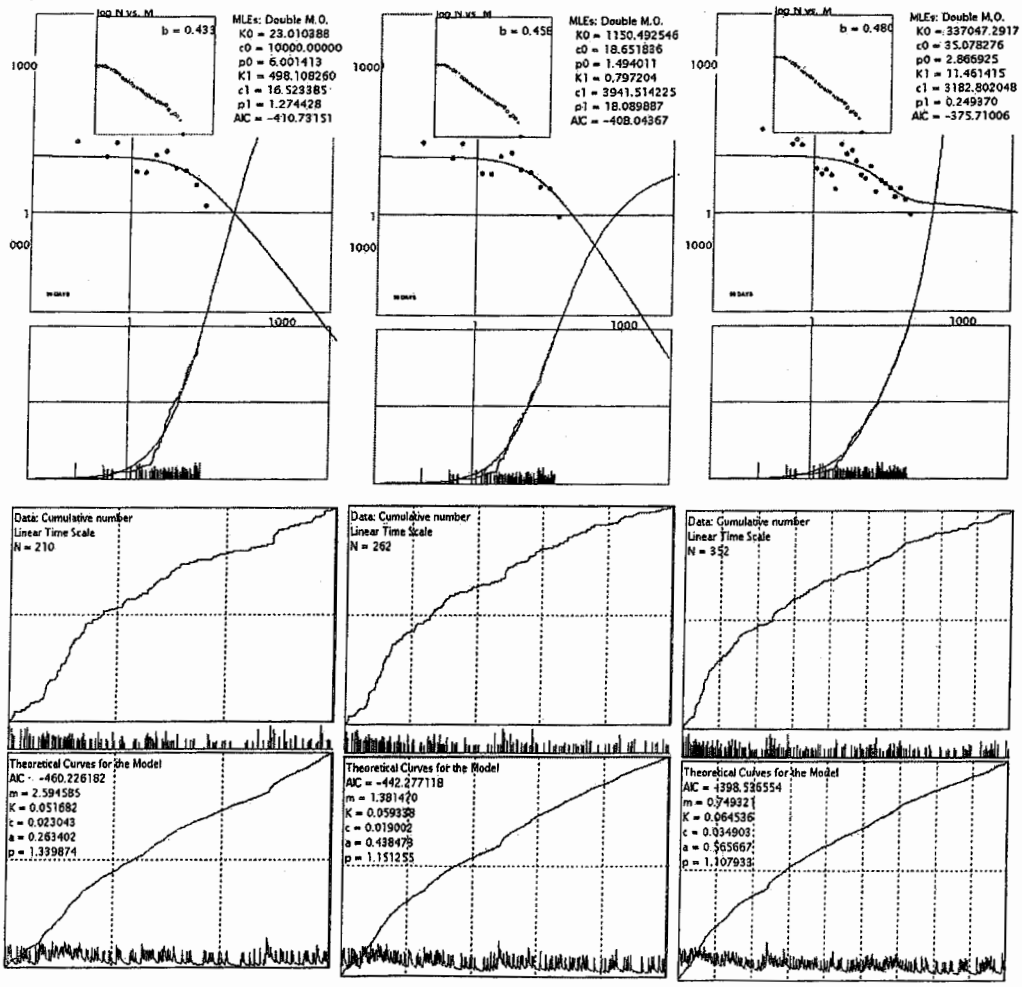

Fig. 6b. Comparison between the fitted results for the direct aftershock period (P2) with the Double Omori (upper plot) and ETAS (lower plot) statistical models for the periods of 30, 50, and 90 days respectively. The upper part of the Double Omori plot shows the Gutenburg-Ritcher curve and the obtained b-value, various model constants and AIC values. The different ETAS model parameters are shown on upper part of its plot.

Table 1: Difference in parameters and the AIC values between models fitted to the direct aftershock data.

No. of Events		30 Days 209	50 Days 261	90 Days 351
Simple Omori Law	AIC	-418.271	-414.158	-382.012
Modified Omori Law	*AIC*	-416.932	-414.340	-380.012
Double Omori Law	*AIC*	-410.732	-408.043	-375.711
ETAS model	*AIC*	-460.226	-442.277	-398.536

Table 2: Parameters estimated from fitting the ETAS model. P12 means a combination of subperiods P1 and P2 into a single subperiod for fitting the ETAS model, and so on.

Period	N	μ	k	c	α	p	b
P1	59	0.001102	0.665721	0.0773998	0.313773	3.000000	0.30288
P2	320	0.830285	0.061725	0.044171	0.632634	1.110708	0.51018
P3	314	0.003624	0.683664	0.125782	0.307475	2.514208	0.50339
P12	379	0.001610	0.142985	0.0181981	0.000000	1.219342	0.46170
P23	633	0.002773	0.477169	0.0849543	1.072798	2.198963	0.51032
P123	692	0.001864	0.606705	0.0188661	0.402697	1.612142	0.48255

Table 3: Comparison between fitting the ETAS model and the Poisson model to the data. AIC is the value for fitting the ETAS model; AICp is the value for fitting the Poisson model; $\Delta AIC = AIC - AIC_P$ represents the AIC gain of the ETAS model from the Poisson model; and $\Delta AIC / N$ means AIC gain per event.

Period	AIC	AIC_P	ΔAIC	$\Delta AIC / N$
P1	559.187266	619.45200	-60.265	-1.022
P2	-355.564249	-343.31977	-12.245	-0.0383
P3	1299.546774	1726.82475	-427.278	-1.361
P12	294.300112	2788.27258	-2493.97	-6.5804
P23	956.542540	1206.96816	-250.4255	-0.39561
P123	1561.433893	4774.59677	-3213.163	-4.6433

Table 4: Comparison between AICs for different divisions of the period.

	P1+2+3	*P12+3*	*P1+23*	*P123*
AIC	1503.169791	1593.846886	1515.729806	1561.433893
$AIC - AIC_{(P123)}$	-58.264102	32.412993	-45.704087	0

These results and those outlined before suggest that even a small region can exist in several different phases of activation with different clustering characteristics as well as different levels of activity at different times. From Fig. 3 it appears that the changes in model parameters may be related to the migration of hypocenter locations to different parts of the fault plane in different periods. The results above can be outlined as a three-stage seismic phase that fits well with the aftershock model proposed by Mogi, (1969). In the first stage, stress is under the critical level and is being built up. The seismic activity is low in this period. This period is referred to as the interseismic stage. The main earthquake occurs after the interseismic period only when the stress levels reach or exceed the critical level. Large clusters or aftershock sequences accompany these forms. This is called the coseismic stage. After most of the accumulated stress is released, the stress field comes into an adjustment period. Seismic activity is still at a high level. Many earthquakes occur in larger clusters, but these clusters are smaller in size and event magnitudes than in the coseismic period. This period may be represented as the post-seismic period.

CONCLUSIONS

Point-process models characterized by parameterized conditional intensity functions are useful tools to investigate seismic activity through a hypocenter catalog. The Dahshour earthquake of October 12, 1992 and its location in particular, came as a surprise for the Egyptian geological and seismological community. It occurred in an area that was considered stable with an apparently simple geological setting and with no observable active surface tectonics. A large number of aftershocks followed the 1992 earthquake but no foreshock was recorded. The absence of microseismic activity before the Cairo earthquake as well as the low b-value (approximately 0.7) (as shown in Fig. 5), given for the area by El-Sayed and Wahlström (1996) manifest a period of seismic quiescence and stress accumulation before a major earthquake. As mentioned above, the surface geology of the epicentral area is covered by loose quaternary sediments with no surface lineaments. Nevertheless, near the 1992 epicentre, El-Shazly et

al., (1979), reported NW-SE and NE-SW fault systems. These are probably due to the complexity of the region, which is affected by the northern Red sea rifting system and by the north-east trending systems such as the Gulf of Aqaba-Levant fault system or the eastern Mediterranean-Cairo-Faiyum system. It is possible that the stress fields of the two systems affected northeastern Egypt (Kulhánek et al., 1992; El-Sayed et al., 1996). The proposed normal-faulting mechanism and the NW-SE oriented strike of the Dahshour earthquake implied that the event occurred along the extension of the stress field of the Red Sea rifting system.

In many cases, an aftershock sequence is more complex than the simple inverse power decay expected by the modified Omori formula. The ETAS model is a generalized version of the modified Omori formula and fits well with various aftershock sequences. In this study, several statistical models were fitted to the data. Among them, the ETAS model fitted the direct aftershocks better than the Omori law, which suggests that the aftershock sequence consisted of multistage clusters. The ETAS model also revealed the existence of a quiescent period before the major earthquake. It showed that there is a clear change of seismicity pattern before and after the immediate aftershock sequence, not only in the mean rate but also in cluster structure. Individually, these changes may not be caused by random fluctuation due to the small number of events in some of the investigated regions, but overall they are beyond the noise level. The change of seismicity pattern suggests a change to the stress field or the mechanical properties of the fault following the main event. The main event was only of magnitude 5.8 but produced a large number of aftershocks and influenced the seismic patterns in the area. These aspects are much like the behavior of large main shocks. It is worth questioning whether the occurrence of such event with strange features in this particular region could be a signal that the seismicity would change in the nearby regions.

ACKNOWLEDGMENTS

This study was partially supported by the Japan Society for the Promotion of Science (JSPS) and carried out as part of a research project under MEXT KAKENHI number 16.04319. The author would like to dedicate this work to people who suffered most in the Dahshour earthquake in Egypt. I wish to thank the National Research Institute of Astronomy and Geophysics (NRIAG), the Egyptian National Seismic Network (ENSN) and Ass. Prof., Dr. K. Abou El-Enean for providing the earthquake catalogs used in this study. We are grateful to Professor Y. Ogata who provided the codes (SASeis2006) for calculating and plotting the seismicity analysis. I thank Drs. H. Takenaka, I. A. Ogunwande, and

J. Deocampo for their helpful suggestions to improve this manuscript to be timely published and Mr. M. Ohshima for his help to plot figures. Some of the figures were generated using the GMT software by P. Wessel and W. H. F. Smith.

REFERENCES

Abou El-Enean, K., 1993. Seismotectonics of the Mediterranean region north of Egypt and Libya. M.Sc. thesis, Faculty of Science, Mansoura University, Egypt.

Abou El-Enean, K., 1997. A study of the seismotectonics of Egypt and relation to the Mediterranean and Red Seas tectonics. Ph. D. Thesis, Faculty of Science, Ain Shams University, Egypt.

Akaike, H., 1977. On entropy maximization principle. In: Krishnaiah, P. R. ed. Applications of statistics. Amsterdam, North Holland. Pp. 27-41.

Badawy, A., 1999. Historical seismicity of Egypt. Acta. Geod. Geophy. Hung., 34 (1-2) 119-135.

Ben-Avraham, Z., Nur, A., and Cello, G., 1987. Active transcurrent fault system along the North African passive margin. Tectonophysics 141, 294-260.

EGSMS (Egyptian Geological Survey and Mining Authority), 1981. Geologic map of Egypt.

EGSMS (Egyptian Geological Survey and Mining Authority), 1993. A preliminary report on the Dahshour Earthquake, 12 October, 1992.

El-Gamili, M., 1982. A geophysical interpretation of a part of the Nile Valley, Egypt based on gravity data. J. Geol. Special Vol. part 2, 101-120.

El-Sayed, A., and Wahlström, R., 1996. Distribution of the energy release, b-value and seismic risk in Egypt. Natural Hazards 13, 133-150.

El-Sayed, A., Wahlström, R., and Kulhánek, O., 1996. Triggering sources for seismicity and distribution of ground acceleration in Egypt. 10th International Seminar on Earthquake Prognostics. Jan 5-10th Cairo, Egypt P 59.

El-Shazly, E.M., Abdel Hady, A.M., El-Ghawaby, A.M., El Kassas, I.A., Khawasik, S.M., El-Rakaiby, M., and Aassy, I.E., 1979. Structural lineament map of Egypt based on Landsat satellite image interpretation field and laboratory investigation. Acad. Sci. Res. Technol., Cairo.

Gross, S.J., Kissilinger, C., 1994. Test of Models of aftershock rate decay. Bull. Seism. Soc. Am., 84, 1571-1579.

Hussein, H., 1999. Source process of the October 12, 1992 Cairo earthquake. Annali Di Geophy. Vol. 42, No. 4, 665-674, August 1999.

Hussein, H., Korrat, I., and Abdel Fattah, A., 1996. The twelve October earthquake, a complex multiple shock; Bull. IISEE, V 30, pp. 9-21.

Kebeasy, R., 1984. Seismicity of Egypt. In: Said, R. (Editor); The Geology of Egypt. A.A., Balkama, Rotterdam, Netherlands.

Kebeasy, R.M., 1990. Seismicity. In: Said, R. (Editor); The Geology of Egypt. A.A., Balkama, Rotterdam, Netherlands, 51-59.

Kulhánek, O., and Korrat, I., El-Sayed, A., 1992. Connection of the Seismicity in the Red Sea and Egypt. Published abstract in the Tenth Annual Meeting of Egyptian Geophysical Society, March 1-3, 1992.

Maamoun, M., Megahed, A., and Allam, A., 1984. Seismicity of Egypt. Bull of HIAG, Vol. IV, Ser. B, 109-160.

Mogi, K., 1969. Some features of recent seismic activity in and near Japan. (2). Activity before and after great earthquakes. Bull. Earthq. Res. Inst. 47, 395−417.

Narteau, C., Shebalin, P., Holschneider, M., 2002. Temporal limits of the power law aftershock decay rate. J. Geophys. Res., 107. (B12): art. no. 2359, Dec 20.

Ogata, Y., 1983. Estimation of the parameters in the modified Omori formula for aftershock frequencies by the maximum likelihood procedure. J. of Physics of the Earth 31, 115-124.

Ogata, Y., 1985. Statistical Models for Earthquake Occurrences and Residual Analysis for Point Processes, Research Memo. (Technical report), No. 288, Inst. Statist. Math., Tokyo.

Ogata, Y., 1988. Statistical models for earthquake occurrence and residual analysis for point process. J. of the American Statistical Association 83, 401.

Ogata, Y., 1989. Statistical models for standard seismicity and detection of anomalies by residual analysis. Tectonophysics 169, 159-174.

Ogata, Y., 1992. Detection of precursory relative quiescence before great earthquakes through a statistical model. J. of Geophys. Res. 97, 19845-19871.

Ogata, Y., 1999. Seismicity Analysis through Point-process Modeling: A Review. Pure Appl. Geophys. 155, 471–507

Omori, F., 1894. On the Aftershocks of Earthquake, J. Coll. Sci. Imp. Univ. Tokyo 7, 111–200.

Said, R., 1981. The River Nile. Springer Verlag. 180 pp.

Utsu, T., 1961. A statistical study on the occurrence of aftershocks. The Geophys. Mag. 30, 526-605.

Utsu, T., 1971. Aftershocks and Earthquake Statistics (III): Analyses of the Distribution of Earthquakes in Magnitude, Time, and Space with Special Consideration to Clustering Characteristics to Earthquake Occurrence (1), J. Faculty Sci., Hokkaido Univ., Ser. VIII 3, 379–441.

Utsu, T., Ogata, Y., and Matsu'ura, R.S., 1995. The centenary of the Omori formula for a decay law of aftershock activity, J. Phys. Earth, 43, 1–33.

Utsu, T., and Seki, A., 1955. Relation between the Area of Aftershock Region and the Energy of the Mainshock, Zisin (J. Seismol. Soc. Japan), Ser. 2, ii 7, 233–240 (in Japanese).

Zhuang, J., 2003. Some applications of point processes in seismicity modelling and prediction, Ph.D. thesis, Grad. Univ. of Adv. Stud., Kanagawa, Japan.